133. Jahrgang (2016), Heft 1, S. 47–61

Austrian Journal of Forest Science
Centralblatt für das gesamte Forstwesen

Generating a digital elevation model using unmanned aerial system for a deep seated rotational landslide on forest cover and vegetation

Digitale Höhenmodelle zur Abschätzung von Hangrutschungen und Waldflächenverteilungen mit unbemannten Flug-Systemen

R. Cuneyt Erenoglu[1]

Key words: Landslide, vegetation, forestry, UAS, digital elevation model, RTK/GNSS

Abstract

Landslides have some effects on the Earth's natural environment. A landslide may change the forest and vegetation borders by releasing downward sediments, forest cover and vegetation. Moreover the diversity of life living in these border areas is adversely affected because of this boundary changing. In addition to the mass movement, heavy rainfall and seismic activity have the important roles to trigger probable landslides prone areas which are to take action. The generation of the current digital elevation model (DEM) is very important immediately after the landslides in order to determine movement direction, character and impacts of the landslide. High resolution DEMs are increasingly generated from photographs acquired with consumer cameras from the unmanned aerial systems (UASs). In this study, we generate DEM reflecting the most current topography of the landslide area on the forestry area, to compare of DEMs from different flight dates and finally with the RTK-GNSS surveys at the landslide borders. In the Biga Peninsula- Turkey, the vegatation is inherently affected by each gravitational mass movement that is one of the major problems endangering the forests. The results showed that the UAS-based DEM generation is higher-accurate in centimeter level, more efficient, faster and lower cost technique

1) Canakkale Onsekiz Mart University, Department of Geomatics Engineering, 17100, Canakkale, Turkey; e-mail: ceren@comu.edu.tr
Tel: +90-286-218 00 18 / 2206; Fax: +90-286-2180541

with respect to the terrestrial surveys. As a final result, this procedure could be used as a tool for quick determination of vegetation and forestry border changes in landslide areas.

1. Introduction

Landslides triggered by heavy rainfall, earthquakes, or human land-use applications, are the widespread impact for mountainous areas (Sidle and Ochiai 2013). Landslides are one of the most studied disturbances in order to explore gradient scales and typescaused by landslides. After a landslide occurredin forests, the below-, on- and above- ground biomass are almost entirely redistributed. The landslides in different location, size and shape has several effects on diversity of animal and play (Garwood et al. 1979). On the other hand, landslides create new habitat for countless species in order to keep their life-cycles (Restrepo et al. 2009).

It is very important to determine the influence of the landslides on forested areas. Many methods have been proposed to study these effects of the landslides such as terrestrial surveys, GPS/GNSS technique, close range and aerial photogrammetry, satellite images and so on. On the other hand, the UAS technology is widely used for various applications due to its pilotless carrier platform. However, remote sensing-based method generally faced a number of problems in generating digital terrain models for the landslides within a dense forest (Sidle and Ochiai 2013). Especially, forest canopy density is one of the major factors in evaluation of landslide and vegetation status within a dense forest using satellite imagery or aerial photos for remote sensing.

The objective of this study is to generate the DEM using UAS to assess the influence of the landslides on forest cover and vegetation within non-dense forest area. For this purpose, the Ambaroba landslide was selected as study area. It is a deep seated rotational landslide, and consists of some transition zones between vegetation and forest. The production of the the current DEM is vital for estimating the influence of the landslide and for determining the width of the transition zone to forest. In addition, the volume changes of the amount of sliding mass depending on the point density were studied using the DEM from the obtained data at different flight dates. The accuracy assessment for the orthophoto from UAS imagery and finally a comparison with the results from other surveys, i.e. RTK/GNSS or tape measurement is performed. To achieve the following tasks, this study was to design and develop a UAS system: (a) Design and implement a UAS system for real-time monitoring of active landslides. (b) Calibrate all the sensors. (c) Connect sensors and geosensors such as GPS/GNSS, gyrocompass, pivoting mouth and digital camera. (d) RTK-GPS/GNSS and CORS surveys for Ground Control Points (GCPs). (e) Test and evaluate the system in a flight experiment. (f) Processing data, 3D modelling, analyzing and comparing the results for the deep seated rotational landslide occurred on vegetation and forest cover.

2. Methodology

Good source data can be accepted as images taken by digital cameras with high resolution for creating man-made objects and digital terrain model. There exists a large number of contributions on techniques and applications of 3D terrain modeling (Brown, 2003; Dequal and Lingua, 2004; Barazzetti et al., 2008). UAS imagery was used for city modeling with high resolution and generation of digital elevation models (Greiwe et al., 2013;Gruen et al., 2013). Furthermore, image based 3D modeling was successfully applied toreconstruct 3D buildingby Haala and Kada 2010. Stereo image processing was performed for submarine ecological studies (Shortis et al., 2009). Image acquisition is a fundamental process for this work. Image based 3D modeling is a process in which information is extracted from sequence of images (Erenoglu et al., 2014). For a large area, only video recording gives better economical solution. A multi-camera setup is designed and developed for video recording of large area (Singh et.al 2013).

In addition to the certain definitions of UAS, the workflow included the photogrammetric flight planning, the calibration stages, image acquisition, quality control, data processing and model generation (Fig. 1). This workflow can specifically be adapted to every type of UAS for all the applications for surveying. Thus, specific tools, such as

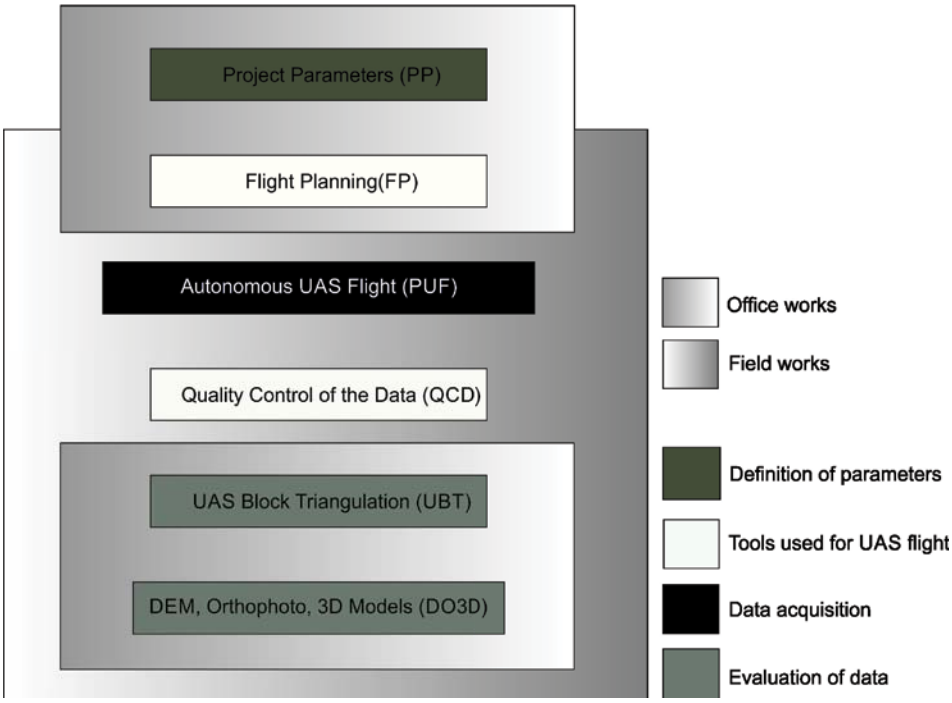

Fig. 1: UAS- based workflow.

design of project parameters and flight planning, are developed as desired. The used workflow allows the combination of field and office work, enabling the first results to be available during the field work for preliminary analysis.

2.1 Eight-totor oktokopter UAS

An octocopter, the UAS Okto XL was used as sensor platform. We preferred okto-rotor system due to its stability during flight with reduced vibration comparing to conventional helicopters. To comply with the requirements for some studies, an okto-rotor open source project has been improved by modifications of the software and the electronic circuit (URL 1).

This micro UAS has an overall weight of about 3.0 kg and a payload of 2.5 kg. This payload includes the camera, the camera mount andthe batteries. As a consequence, a lightweight mirrorless digital camera would allow the use of higher capacity and heavier batteries which would increase the flight time. The used configuration nearly allowed approximately 45 minutes of the optimum flight time. The other technical data of Oktokopter XL can be seen in Table 1.

Dimensions	73 cm x 73 cm x 36 cm
Payload	2500 g
Max. altitude	100 m (Line of sight)
Max. distance	100 m (Line of sight)
Flight time	45 min
Realisticflight time	18-28 min
Telemetrydata	Voltage, capacity, current, altitude, distance, direction, speed, temperature

Table 1: Technical Specifications of UAS Okto XL

2.2 Digital camera-systems

For optimum flight time, the eight-rotor UAS should be equipped with lightweight low-cost mirrorless digital camera, which support manual camera settings. In this study, we used Canon EOS-M Mirrorless Digital Camera. For all flights the camera settings were fixed to ISO 200 at F 2.8 and a focus of 18 mm. These settings enabled an average shutter speed of 1/800 s which was necessary to avoid blurred photographs. Note that we used a shutter that can be controlled by remote control.

2.3 Calibration scheme

High accurate digital surface modeling requires well calibrated cameras. In order to calibrate mirrorless digital camera, we used the PhotoModeler Scanner software tool

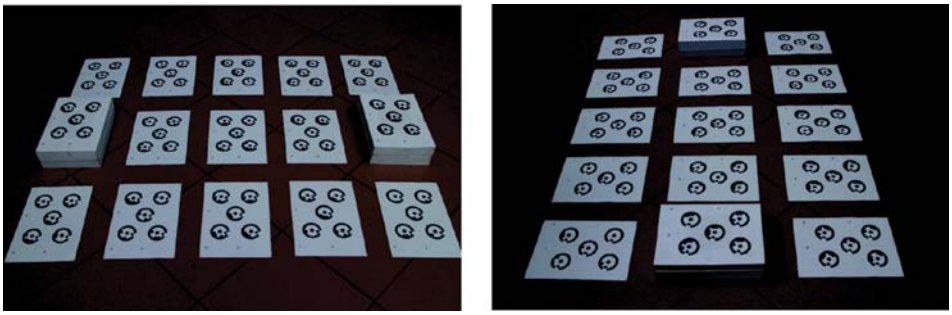

Fig. 2: Calibration sheets used in this study

Calibration Parameter		Value (mm)	Deviation (mm)
Focal length		18.697047	0.003
Principal Points	Xp	11.632606	0.005
	Yp	7.782084	0.006
Format Width (Fw)		22.768255	0.003
Format Height (Fh)		15.163800	
Radial Distortions	K1	4.947e-004	3.9e-006
	K2	-8.669e-007	2.9e-008
	K3	0.000e+000	
Decentering Distortions	P1	-6.402e-005	3.7e-006
	P2	1.169e-004	4.1e-006

Table 2: Camera calibration report

for producing 3D modeling (URL 2). It consists of a developed camera calibration function that defines information about the used camera that improves accuracy for the modelling studies.

It can easily calculate principal point, focal length, lens distortion and format aspect ratio of the camera. For camera calibration, we used flat sheets of target dots by taking the photos of straight, right oblique, left oblique from four different directions, separately (Figure 2). We performed calibration process with a total of 20 photos. Finally, the PhotoModeler Scanner generated of a file including the calibration parameters, that are focal length, format size, principal point and radial and decentering distortion of the lens (Table 2).

2.4 Study area

In this research, the generation of the digital elevation model that has been used in a deep seated rotational Ambaroba landslide, which is located in the Biga Peninsula, Canakkale, NW Turkey. The study site is covered by vegetation within non-dense fo-

rest area, and consists of some transition zones between vegetation and forest. Furthermore, the areas in the south and west sides of landslide are mostly forested.

Ambaroba Village has a hot mediterranean climate that is mild with moderate seasonality. While winters experience moderate temperatures and changeable, rainy weather due to the polar front, summers are dry and hot due to the domination of subtropical high pressure systems. The landslide is located on the North-facing slope of the Ambaroba Basin. This landslide is one of the persistently active landslides at Biga Peninsula, Canakkale since the 2000s. Several destructive reactivations have occurred between 2003 and 2009, resulting in damage barns and buildings (Erenoglu et al., 2014). The thicken towards to the west in the downslope direction and the average depth of slip surface is about 11 m. Ambaroba landslide is classified as a slow flowing gravitional mass movement due to its low velocities (max 0.1 meter per a day).

2.5 Data acquisition/ photogrammetric flight

The UAS-Okto XL used to fly in an autonomous mode. Before flight mission the operator needs to test all the electronic parts of UAS whether every part is working properly. For a successful flight operation, it is very critical to be aware of potential problems on UAS. It is required that the GPS onboard, rudder, elevator and main frame, digital camera, camera mount, propeller, electronic speed controller and remote controller should be checked before the flight. A suitable location is provided for launching operation after all tests have been performed. Note that the autonomous flight mission was preferred to capture images by digital camera in this study. Two people operated the autonomous UAS flight, e.g. ground crew station and operator. In this study, the operator was responsible to control UAS during launching and landing operation to avoid any damages on UAS. Ground crew station performed to monitor flight line, data link between UAS and computer, number of satellite, real time battery status, UAS position and attitude at the ground station. For flight planning step, the working area and suitable locations for starting and landing were chosen. The flight planning included 30 predefined waypoints in Google KML formats (Fig. 3(a)).The distance between 6 parallelneighbouring flight lines was planned with 30 m which equates strip and across-strip overlaps of about 80% and 60%, respectively. Note that during the flight it was especially focused on the section where the vegetation is dense.

After that, two sets of UAS-acquired photographs covering the sliding area were taken on two different flight dates (February 20th 2014 and August 2nd 2014) in order to generate individual digital elevation models for these flight dates and to compare them. The quadrotor was launched to the maximum flight altitude of about 80 m. All images were taken using shooter of remote controller and First Person View (FPV) flying mode. The photos were taken at 30 m, 50 m and 80 m heights from the top level of the landslide, seperately. Each photo covers different size of photo depending on the flight height. The flight mission took about 25 minutes to complete. A number of

Fig. 3: (a) Predefined waypoints for flight plan, **(b)** Some examples of taken aerial images by UAS, **(c)** Surveying mark with plus-shaped, **(d)** RTK/GNSS surveyings on the points, **(e)** Check points on the ground, **(f)** Check points on the image.

the images were captured to cover the whole working area near forest cover and vegetation (Fig. 3(b)). The covered area of the acquired photographs was downloaded, checked and stored as 16 bit TIFFs for further processing on-site after each flight.

2.6 RTK/GNSS surveying for ground control points

For the process of georeferencing an image to be produced, the landslide area was covered with 16 ground control points for each flight date. These points that are used to project 3D landslide model into local coordinate system were marked with plus-shaped. Figures 3(c), 3(d), 3(e) and 3(f) shows marking with plus-shaped, RTK/GNSS surveyings on the points, check points on the ground and on the image, respectively. Furthermore, 8 check points were established especially on the characteristics border regions of the landslide in order to perform accuracy assessment of UAS based 3D modelling. Moreover, the check points were used for determining the expansion of the landslide boundary, i.e. cracks and slots. The RTK/GNSS surveyings were also done for collecting the landslide check points in order to obtain their 3D coordinates.

3. Data processing and results

In this study, all acquired images were in good quality and they were being preceded for the processing. During the flight there was not a considerable wind, approximately 2 m/s. Note that some quality problem may be arised due to color balancing error and blurring image during flight operation. A new flight would be planned to be

performedif the quality of the images were bad. The process of 3D modelling consists of stages of interior orientation, relative orientation, aerial triangulation and bundle adjustment. Herein, two individual data were obtained for on two different flight dates (February 20th 2014 and August 2nd 2014). In this section, the obtained results relating the 3D model generation were given only for the flight on February 20th 2014 due to the lack of space.

Before the image processing, interior orientation was successfully defined in the camera calibration stage mentioned before. Image correlation was used as relative orientation for transferring the tie points between images. In order to align all images taken during UAS flight in the same condition, tie points were utilized.

After data acquisition, the next step is image 3D data processing. In order to product 3D digital terrain model of the landslide, the UAS images were processed using PhotoModeler Scanner Software (EOS Systems). It has been well developed for all the stage of image processing such as camera calibration, triangulating image blocks using measured tie points, digitizing and texturing 3D features.

First, all photos were processed to get the image planes from UAS photos and the image frustum plane. As shown the image plane and image plane frustums in Fig. 4, the linear path are almost parallel to each other. The camera's principal axis is the line perpendicular to the image plane that passes through the pinhole. Its intersection with the image plane is referred to as the „principal point" illustrated in Fig. 4. Image plan frustum is the region of space in the modeled world that may appear on the screen; it is the field of view of the used camera. Using the distortion functions obtained with the pre-calibration, all the photos were resampled. Thus, more realistic terrain view was rectified after distortion correction. Using 167 of the 244 photos, a total amount of 7456 sets of tie points in eachf overlapped pairs of photos were suc-

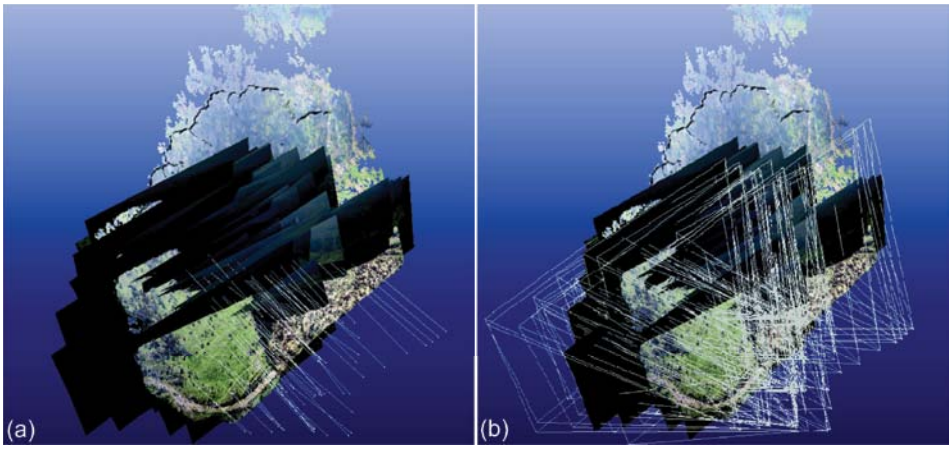

Fig. 4: (a) Image plane, **(b)** Image plane frustums

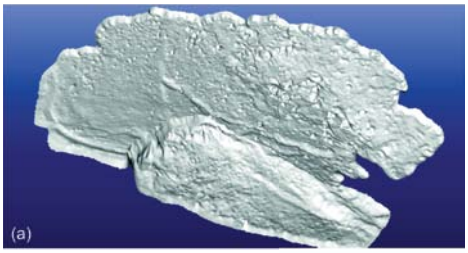

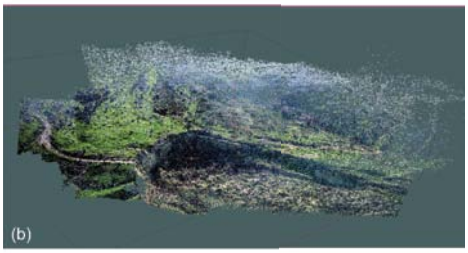

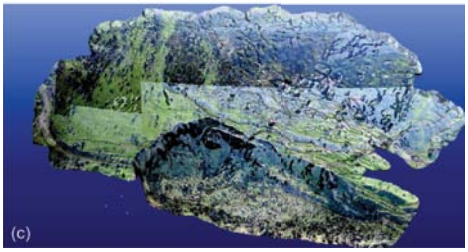

Fig. 5: (a) Single color mesh produced from the process, **(b)** 3D point clouds with exact color, **(c)** Triangle surface included by the texture model

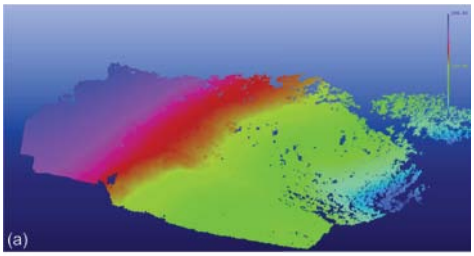

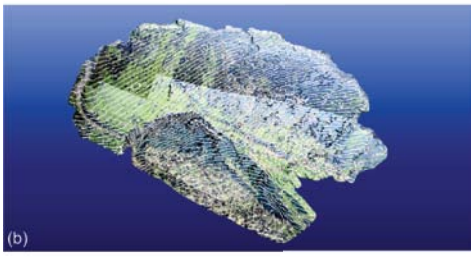

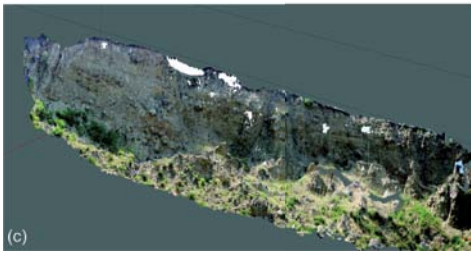

Fig. 6: (a) Digital Elevation Model interpolated with a 10 cm grid, **(b)** Ortho-image product with the contour lines, **(c)** Comparison between DEMs at different flight dates.

cessfully identified at the relative orientation process using the software. After the-relative orientation process, the white point cloud and single color mesh models of the landslide were produced in the PhotoModeler Scanner software. The produced single color mesh can be seen in Fig. 5(a). Note that some areas in white point cloud are missing in single color mesh. The inconsistent data is automatically missed, so that the produced model can then be fitted more accurately to the input data.

Then, 3D point clouds with exact color from photos were obtained (Fig. 5(b)). Here, the number of point cloud significantly increased using more efficient methods of feature matching techniques. The dense point cloud models of the Ambaroba Landslide were given for the flight on February 20th 2014. It produces more details of the landslide than the white point cloud and single color mesh.

After the procedures of adjustment and projection to the UTM system using the GCPs, a surface including 76548 triangles was generated based on the 3D points after edition and noise filtering by the software (Fig. 5(c)).

Quantity	X coordinate	Y coordinate	Z coordinate
Min.	4451924.587	533368.268	230.619
Max.	4452121.406	533510.907	281.659
Range	196.819	142.639	51.040
Mean	4451972.720	533454.895	265.717
Median	4451967.355	533472.868	269.072
Tile of 25%	4451943.628	533424.775	257.178
Tile of 75%	4451995.413	533485.772	274.119
St. Dev.	33.273	40.187	10.414
Variance	1107.093	1614.995	108.451

Table 3: Univariate Statistics of the point cloud

Univariate statistics of the point cloud were studied in order to find out the statistical properties of the obtained data. Each coordinate component was taken as a seperate data point. Table 3 shows some univariate statistics of the point cloud. Furthermore, the quantiles were calculated for the cumulative probabilities of 0.25, 0.5, 0.75, and 0.975. The autocorrelation procedure of the PhotoModeler Scanner provided a well distributed data due to normal distributed point positions of data cloud.

DEM with the grid size of 10 cm was produced using the procedure of regular grid since the triangle surface points have some irregular concentrations (Fig. 6(a)). Note that the new surface was interpolated for all points in each 0.10 m by the radial basis function (Webster and Oliver, 1990). Finally, the ortho-image presents an important product to show soil deformations of landslide area including vegetations and forest-cover as well as surface topography and other cartographic properties. For Ambaroba Landslide, the ortho-photo product with the contour lines was generated from the flight on February 20th 2014 (Fig. 6(b)). Herein, the contours lines with an interval of 1 m were obtained by intersecting the DEM and a set of 1-m interval parallel planes to the horizontal plane.

Up to this point, the obtained models were presented only for the flight at 50 m height due to the lack of space. In addition, the similar workflow is applied to the data for the other flight heights, i.e. 80 m and 30 m. Different spatial resolutions were obtained at different flight heights as accuracy criteria about the level of detail of the orthoptohos generated in this study. Note that the results of the geometric accuracy assessment based on the locations of the ground control points surveyed in the field work. The Root Mean Squared Errors (RMSE) and standard deviations are 0.29 ± 0.15 for 80 m, 0.25 ± 0.13 for 50 m and 0.20 ± 0.18 for 30 m in centimeter level. As a result, the lower flight height provided higher accurate orthophoto product using a low cost UAS and camera system. Two individual DEMs were generated for two different flight dates. The final analysis of this study involves volume determination of landslide and soil loss. In general, the soil loss in the landslide area can be calculated by subtracting DEMs obtained from the data at different dates. Surface volume tools are available in ArcGIS 9.3 for calculating surface volume automatically. In order to make

a comparison between DEMs for different flight dates, the volume of soil loss was calculated by subtracting the two different surface volumes for the main scarp of the Ambaroba Landslide (Fig. 6(c)).

The difference between the topography is shown in white color. It is clear that there is a significant soil loss after 6 months between the observation periods due to the gravitational mass movement. Moreover, a majority of soil loss occurred in top region of the landslide including forest cover and vegetation. The results from ArcGIS 9.3 showed that the sum of soil loss of the Ambaroba Landslide is 10.65 m^3 and the area of landslide is 1.2417 m^2 in top region.

4. Discussion

We evaluate the quality and accuracy of UAS-based product, i.e. orthophoto by comparing them with control measurements made with RTK/GNSS measurements on the ground on February 20th 2014. The orthophoto was realized using the texture of the 3D landslide model. For this purpose, the planar and vertical comparisons are performed by control surveys of ground control points that are clearly identifiable on orthophotos. The statistics of these differences are used to evaluate the accuracy of

GCP #	XY error (m)	Z error (m)	GCP #	XY error (m)	Z error (m)
1	0.020	0.040	9	0.019	-0.032
2	0.040	0.061	10	0.025	-0.030
3	0.024	0.023	11	0.023	-0.014
4	0.020	-0.002	12	0.029	-0.009
5	0.047	0.041	13	0.022	0.015
6	0.023	0.005	14	0.005	0.042
7	0.025	-0.041	15	0.015	0.027
8	0.015	0.022	16	0.038	-0.042

Table 4: The surveyed errors between UAS- orthophoto and RTK/GNSS for the GCPs

CheckPoint #	UAS- Orthophoto Coordinates			RTK/GNSS Coordinates		
	X (m)	Y (m)	Z (m)	X (m)	Y (m)	Z (m)
C1	533376.512	4451992.055	249.606	533376.514	4451992.044	249.634
C2	533381.032	4451996.189	250.068	533381.037	4451996.179	250.048
C3	533380.298	4451987.194	250.757	533380.291	4451987.218	250.793
C4	533383.234	4451990.193	251.428	533383.228	4451990.179	251.452
C5	533382.940	4451983.354	251.928	533382.935	4451983.380	251.952
C6	533386.281	4451984.400	252.792	533386.262	4451984.405	252.794
C7	533384.798	4451978.434	252.345	533384.807	4451978.424	252.359
C8	533392.070	4451977.903	253.715	533392.046	4451977.910	253.697

Table 5: The UAS-orthophoto and RTK/GNSS coordinates of check points

UAS-based products. The 3D coordinates of each of the 16 GCPs were calculated from UAS-based orthophoto and compared with the coordinates measured with RTK/GNSS. The UAS-model coordinates were derived from the producting geo-referenced orthophoto. The difference between UAS-orthophoto coordinates and RTK/GNSS coordinates of the 16 GCPs is shown in Table 4.

8 check points were established and surveyed by UAS- technology and also RTK/GNSS to determine the landslide borders. Table 5 shows the coordinates of 8 check points obtained by these methods. Then, the root mean squares (rms) for X, Y, Z coordinates were computed by:

$$RMS_X = \sqrt{\frac{1}{n}\sum_{i=1}^{n}(X_{ORTHO\,i} - X_{RTK\,i})^2} \quad (1)$$

$$RMS_Y = \sqrt{\frac{1}{n}\sum_{i=1}^{n}(Y_{ORTHO\,i} - Y_{RTK\,i})^2} \quad (2)$$

$$RMS_Z = \sqrt{\frac{1}{n}\sum_{i=1}^{n}(Z_{ORTHO\,i} - Z_{RTK\,i})^2} \quad (3)$$

The RMS values are obtained as 12 mm, 15.1 mm and 22.8 mm for X, Y and Z coordinates, respectively. It is clear that the coordinates obtained from UAS- orthophoto and RTK/GNSS are highly consistent with each other.

Finally, it is aimed to assess the availability of the coordinates from UAS-orthophoto and to compare its results with the ones by RTK/GNSS surveying under some changing environmental conditions due to landslides. For this purpose, 8 checkpoints were established just behind the landslide: 4 points at the lower side of landslide (C2, C4, C6 and C8) and 4 points on the sliding crack near the vegetation area (C1, C3, C5 and C7) on February 20th 2014. First, the distances were measured by a steel measu-

Line	Model Measurement (m)	Tape Measurement (m)	Difference (m)
C1-C2	6.14	6.17	0.03
C1-C3	6.28	6.28	0.00
C2-C4	6.53	6.54	0.01
C3-C4	4.24	4.23	0.01
C3-C5	4.80	4.81	0.01
C4-C6	6.68	6.70	0.02
C5-C6	3.60	3.61	0.01
C5-C7	5.28	5.30	0.02
C6-C8	8.74	8.75	0.01
C7-C8	7.40	7.40	0.00

Table 6: Accuracy result analysis for 3D model

ring tape from each one to the other. Then, the same distances were also obtained from the orthophoto. The lengths of distances obtained by both approaches can be seen at Table 6. The orthophoto product and the surveyed distances clearly show that both lines, i.e. C1, C3, C5, C7 and C2, C4, C6, C8, has almost overlap. Moreover, the results of UAS- model measurements were compared against results from tape surveying as a further quality check. The difference results are close to each other in the cm level, up to 3 cm. As a consequently, for landslide areas near the vegetation cover, it was proven that the UAS-based orthophoto products has sufficient accuracy in terms of point positioning compared to the ones by terrestrial tape measurements. Therefore, the usage of UAS-based techniques should be favoured for modelling the impacts of active landslides on the vegetation and forest covers since it provides accuracy, efficiency and economy (Erenoglu, 2015).

The forest boundary line consists of the check points of C1, C3, C5 and C7. The other check points (C2, C4, C6 and C8) are on subsidence line of the landslide. The average current values of the forest line and the subsidence line are 51.159 m and 52.001 m, respectively. When considering the topography in Fig. 12, the main reason for the significant change in height difference (about 84 cm) is the massive landslides along very short distance. Moreover, the analysis clearly showed that 83.062 m² of surface land mass among these points was significantly descended about 0.8 m nearly at the border of the forest. This result is one of the most striking remarks of this study.

5. Conclusions

In this study, we use the UAS based terrain model production to estimate the impacts of active landslides at the forest line and vegetation. The workflow included the calibration stages, UAS based image acquisition, surveying of ground control points, image processing, model creation, textured model generation, digital surface model extraction and accuracy assessment.

By applying UAS, the DEMs could be generated more efficiently and accurately with respect to the GPS/GNSS based positioning and the terrestrial techniques for the landslides. The results showed that it was possible to determine current status of the landslide and changes in transition zone to the forest using UAS technology. The vegetation loss on the transition zones can be successfully obtained by subtracting DEMs obtained from the data at different dates.

The most important achievement of our work was to get accurate orthophoto products using a low cost UAS and camera system. The height of flight and exact number of ground control point are required for a good quality DEM. For orthophoto products, achievable accuracy varies depending on the height of the flight. Furthermore, the analysis of this study showed that UAS- based products provided the accurate location information with respect to the conventional approaches, e.g. RTK/GNSS and tape measurements. The resulting DEM using UAS technology is as accurate as

RTK/GNSS, is much faster and provides a richer representation of currect topography and geography. Moreover, it is important to use UAS-based surveying for modelling location, size and shape of the landslides near vegetation and forest coverin order to keep diversity of animal and play. Finally, the analysis will be most accurately and consistently determined using UAS-based surveying before the creation of geographical information system, but can also be approximately in the vegetation and forest cover.

Acknowledgements

The author is very grateful to the editor and two anonymous reviewers for their constructive and critical comments which improved the earlier draft significantly. Furthermore, the author greatly appreciates Dr. Ozgun Akcay for field assistance during the aerial survey. Google Earth picture was used as Fig 3. This study is supported by TUBITAK (The Scientific and Technological Research Council of Turkey) with the project number 112Y336.

References

Barazzetti, L., Brovelli, M., Scaioni, M., 2008: Generation of true-orthophotos with LiDAR dense digital surface models, The Photogrammetric Journal of Finland 21(1), p. 26-34.

Brown, J., 2003:Aspects on true-orthophoto production. In Proceedings of the Phot. Week'03.Wichmann, Stuttgart, Germany 2003, p.205-214.

Dequal, S., Lingua, A., 2004: True orthophoto of the whole town of Turin, International Archives of Photogrammetry, Remote Sensing and Spatial Information Sciences 34(5/C15), p. 263-268.

Erenoglu R. C., Akcay O., Erenoglu O., 2015: Estimating of landslide by repeated GPS/GNSS measurements in the Ambaroba Region, Canakkale, NW Turkey. In Proceedings of the International Symposium on Modern Technologies, Education and Professional Practice in Geodesy and Related Fields, Sofia, Bulgaria 2015.

Erenoglu, R. C., Akcay, O., Erenoglu, O., Uluocak, E. S., Karaca, Z., 2014: UAV based monitoring of Adatepe Landslide, Canakkale, NW Turkey. In Proceedings of the FIG Congress 2014, Engaging the Challenges, Enhancing the Relevance, Kuala Lumpur, Malaysia 2014.

Haala, N., Kada, M., 2010: An update on automatic 3D building reconstruction, ISPRS Journal of Photogrammetry and RemoteSensing 65(6), p. 570-580.

Garwood, N. C. et al., 1979: Earthquake-caused landslides: a major disturbance in tropical forests, Science 205, p. 997–999.

Greiwe, A., Gehrke, R., 2013: Foveon Chip oder Bayer Pattern - geeignete Sensoren zur Aerophotogrammetriemit AUS. In: Photogrammetrie, Laserscanning, Optische 3D-Messtechnik -Beiträge der Oldenburger 3D-Tage 2013 (Luhmann,T., Müller, C., ed.), p. 334-343.

Gruen, A., Huang,X., Qin,R., Du,T.,Fang,W.,Boavida,J., Oliveira, A., 2013: Joint processing of UAV imagery and terrestrial mobile mapping system data for very high resolution city modeling, ISPRS-International Archives of the Photogrammetry, Remote Sensing and Spatial Information Sciences 1(2), p. 175-182.

Restrepo, C. et al., 2009:Landslidingandits multi-scaleinfluences on mountainscapes, BioScience 59,p. 685-698.

Shortis, M., Harvey, E. S., Abdo, D., 2009: A review of underwaterstereo-image measurement for marine biology and ecology applications, Oceanogr Mar Biol AnnuRev 47,p. 257-292.

Sidle, R. C.,Ochiai, H., 2013:Landslides: processes, prediction, andlanduse, Water Resources Monograph 18. Washington, DC: American Geophysical Union.

Singh, R., Qureshi, Q., Sankar, K., Krausman, P. R., Goyal, S. P., 2013: Use of camera traps to determine dispersal of tigers in semi-arid landscape, western India, J Arid Environ 98, p.105-108.

Webster, R., Oliver, M. A., 1990: Statistical methods in soil and land resources survey, Oxford University Press.

URL 1: "Mikrokopter Drone." Internet: www.mikrokopter.de/en/home, Oct. 25, 2009 [May 15, 2015].

URL 2: "PhotoModeler Scanner." Internet: www.photomodeler.com/products/scanner/default.html, Jan. 25, 2010 [May 10, 2015].